South African Journal of Botany 180 (2025) 668–679

Contents lists available at ScienceDirect

South African Journal of Botany

journal homepage: www.elsevier.com/locate/sajb

Phenolic compounds profile and hypoglycaemic, anti-inflammatory and antioxidant properties of aqueous leaf extract of *Androstachys johnsonii* Prain: *In vitro* study

Murendeni Nethengwe[a], Nasifu Kerebba[b,d], Kunle Okaiyeto[a], Chinyerum S. Opuwari[c], Oluwafemi O. Oguntibeju[a,*]

[a] *Phytomedicine and Phytochemistry Group, Department of Biomedical Sciences, Faculty of Health and Wellness Sciences, Cape Peninsula University of Technology, Bellville 7535, South Africa*
[b] *Department of Chemistry, Makerere University, Kampala 7062, Uganda*
[c] *Department of Medical Biosciences, University of the Western Cape, Bellville, South Africa*
[d] *Department of Physical Sciences, Kampala International University, Kampala, Uganda*

ARTICLE INFO

Article History:
Received 21 October 2024
Revised 6 March 2025
Accepted 24 March 2025
Available online 1 April 2025

Edited by: Dr A. Andrade-Cetto

Keywords:
Antioxidants
Diabetes mellitus
Hyperglycaemia
Inflammation
Phenolic compounds

ABSTRACT

Androstachys johnsonii Prain has been identified through ethnobotanical studies as a medicinal plant used in traditional medicine to treat medical complications, including diabetes mellitus (DM). The development of DM complications involves hyperglycaemia and excessive production of free radicals and inflammatory cytokines. This study investigates the hypoglycaemic, antioxidant, and anti-inflammatory properties of the aqueous extract of *A. johnsonii*, to reveal the possible pathways through which the extract can possibly treat DM complications. A total of 34 phenolic compounds (majorly flavonoids) was identified in the plant extract through the Ultra-High Performance Liquid Chromatography Mass Spectrometry (UHPLC-MS) analysis. Total polyphenols were 403.28 ± 12.75 mg gallic acid equivalent (GAE)/g with 88.35 ± 2.16 mg catechin equivalent (CE)/g of flavanols and 6.96 ± 3.10 mg quercetin equivalent (QE)/g flavonols. For antioxidant capacity determination, ferric reducing antioxidant power (FRAP) (1342.68 ± 3.41 mg ascorbic acid equivalent (AAE)/g), 2,2-diphenyl-1-pycrylhydrazyl (DPPH) (571.57 ± 0.55 mg Trolox equivalent (TE)/g), and Trolox equivalent antioxidant capacity (TEAC) (478.88±0.09 mg Trolox equivalent (TE)/g) values were obtained. The extract demonstrated a concentration-dependent anti-inflammatory activity on RAW macrophage cells. The highest concentration of the extract increased glucose uptake and utilisation in C3A hepatocarcinoma cells. The extract showed a significant concentration-dependent ($P < 0.05$) increase in α-glucosidase inhibition and a significantly ($P < 0.05$) lower pancreatic lipase inhibition. These results suggest the potential therapeutic effect of *A. johnsonii* in the treatment of DM.

© 2025 The Authors. Published by Elsevier B.V. on behalf of SAAB. This is an open access article under the CC BY-NC-ND license (http://creativecommons.org/licenses/by-nc-nd/4.0/)

1. Introduction

Hyperglycaemia is a main characteristic of diabetes mellitus (DM) (Yao et al., 2023). DM is a global concern due to its increased prevalence and an increase in mortality rate (Bodke et al., 2023; Ye et al., 2023). Currently, 1 in 11 adults globally have been diagnosed with DM (commonly type 2 diabetes mellitus) (Fenta et al., 2023). It has also been estimated that 642 million people worldwide will be affected by DM in 2040 (Bodke et al., 2023). Although the pathogenesis of DM arises from reduced glycaemic control and impaired glucose metabolism, several other factors such as oxidative stress and inflammation are implicated in the development of DM complications (Jubaidi et al., 2021). During the development of DM, the interaction of excessive glucose with biomolecules leads to the formation of advanced glycation end-products, and subsequent tissue damage (Khalid et al., 2022). Chronic inflammation is one of the instigators of medical complications accompanying DM (Ramesh et al., 2022; Rohm et al., 2022). Glucotoxicity leads to the upregulation of the nuclear factor erythroid 2-related factor (NRF2) which causes immune cells infiltration and further damage caused by excessive production of inflammatory cytokines (Cai et al., 2023). Hyperglycaemic complications also include the excessive production of reactive oxidative species and compromised antioxidant system leading to oxidative stress (Bhatti et al., 2022). The reaction of ROS with biomolecules causes oxidation and subsequent damage which leads to apoptosis, alteration, and deactivation of biomolecules (Liu et al., 2022b).

* Corresponding author at: Department of Biomedical Sciences, Cape Peninsula University of Technology, Bellville 7535, South Africa.
E-mail address: OguntibejuO@cput.ac.za (O.O. Oguntibeju).

https://doi.org/10.1016/j.sajb.2025.03.047
0254-6299/© 2025 The Authors. Published by Elsevier B.V. on behalf of SAAB. This is an open access article under the CC BY-NC-ND license (http://creativecommons.org/licenses/by-nc-nd/4.0/)

Oxidative stress is also directly linked to chronic inflammation and exacerbation of DM complications (Sahakyan et al., 2022). It is therefore evident that the direct amelioration of both oxidative stress and inflammation, and the reduction of blood glucose levels is paramount in the treatment of DM.

The modern treatment of DM includes the use of hypoglycaemic synthetic drugs (Haq et al., 2021). As an example, the use of acarbose has also been linked with its hypoglycaemic effect through the inhibition of α-glucosidase and α-amylase (Saddique et al., 2022). Regardless of the effectiveness of synthetic drugs, traditional medicine has drawn scientific focus due to the review of the adverse effects and economical concerns that arise from the use of synthetic drugs (Blahova et al., 2021; Nguyen et al., 2022). Currently, several ethnobotanical studies have been conducted in search of medicinal plants that are effective in the treatment of DM (Amoo et al., 2022; Andrade et al., 2020; Bouyahya et al., 2021). Previous studies show that the pharmacological effect of medicinal plants is linked to the bioactive compounds constituted in the plants (Khan et al., 2022; Rahman et al., 2022; Yang et al., 2021b). The isolation of individual compounds with respect to their targets and mechanisms of action is of interest investigating therapeutic alternatives in the treatment of diseases (Ercan and Doğru, 2022). However, medicinal plants contain several phenolic compounds that can possibly act synergistically. Phenolic compounds in plants are known to have hypoglycaemic, antioxidant and anti-inflammatory properties (Pieczykolan et al., 2021), hence their use in the treatment of various disease conditions including DM. In line with the discovery of efficacious medicinal plants, several studies have been conducted to investigate the chemical composition of plants, and their beneficial effects in the treatment of medical complications (Kiliccioglu et al., 2024; Shoukat et al., 2024).

Androstachys johnsonii Prain, also known as Lebombo ironwood, is a relatively tall (up to 15 m tall), green plant belonging to the Picrodendraceae family (Mfotie Njoya et al., 2024). *A. johnsonii* originates from the Africa and Madagascar, commonly known as a source of yellow wood (Magalhães, 2021). The leaves, roots, and barks of *A. johnsonii* are used in traditional medicine for the treatment of infections, stomach aches, DM, and as an aphrodisiac for men (Mfotie Njoya et al., 2024). Phenolic compounds such as catechins, bioflavonoids, gallic acid, tannins, quinic acid were previously identified in the leaves of *A. johnsonii* (Mfotie Njoya et al., 2024). A similar biological study revealed the antifungal effect of *A. johnsonii* roots, barks, and leaves with association to the presence of catechin as a bioactive compound (Molotja et al., 2011). Although ethnobotanical studies have identified the plant as a commonly used treatment for DM, only very scanty studies have revealed the action of the plant and its bioactive compounds possibly responsible for its effect. Therefore, this study was designed to comprehensively investigate the potential effect of *A. johnsonii* in reducing glucose levels and ameliorating oxidative stress and inflammation.

2. Materials and methods

2.1. Chemicals

The following chemicals and reagents were purchased from Sigma-Aldrich; Dimethyl sulfoxide (DMSO), α-glucosidase (from *Saccharomyces cereviciae*), Lipase from porcine pancreas, *p*-nitrophenyl palmitate (pNPP), dibasic sodium phosphate, monobasic sodium phosphate, acarbose, Tris–HCl, 4-nitrophenyl beta-d-glucoside (pNPG), triton-X100, isopropanol, sodium deoxycholate ferric reducing antioxidant power (FRAP) reagent, 2,2-diphenyl-1-pycrylhydrazyl (DPPH) reagent, 2,2′-azino-bis (3-ethylbenzothiazoline-6-sulfonic acid (ABTS), ascorbic acid, gallic, acid, atropine, catechin. minimal essential medium (MEM) and phosphate buffered saline (PBS) without Ca^{2+} and Mg^{2+} were purchased from Cytiva, in Marlborough, MA, USA. Lipopolysaccharide (LPS), aminoguanidine and RPMI1640 culture medium were purchased from GE Healthcare Life Sciences, Logan, UT, USA. Sulphanilamide and NED Solutions were purchased from Promega. Penicillin/streptomycin, foetal bovine serum and non-essential amino acids were purchased from Biowest in Nuaillè, France. orlistat, RPMI-1640 Medium, RAW 264.7 mouse macrophages were purchased from Cellonex, South Africa. C3A hepatocarcinoma cells were purchased from ATCC, USA.

2.2. Plant material collection and preparation

The *A.johnsonii* plant was identified at the Brackenridgea Nature Reserve in Thengwe, Limpopo, South Africa. The leaves of the plant were harvested and authenticated at the University of Venda, by Prof. Tshisikhawe (voucher number: MNU001/10/22) and a specimen was kept at the herbarium at the University of Venda. An aqueous leaf extract was prepared from the leaves of *A. johnsonii*. The leaves were dried in the shade for 3 days and hand-crushed to smaller particles. The leaves were then blended into a powder. The powder was weighed and soaked in 100 °C hot distilled water at a ratio of 1:10. The mixture was left overnight (24 h). Extraction of the liquid in the mixture was performed using size 2 and 3 filters and the filtrate was freeze dried overnight. The extract was kept in a −20 °C freezer.

2.3. Ultra-High performance liquid chromatography mass spectrophotometry (UHPLC-MS) phenolic compound profiling

Phytochemical profiling of aqueous leaf extract of *A. johnsonii* was performed using a mass spectrometer, Water Synapt G2 Quadrupole time-of-flight (QTOF) coupled with a Waters Acquity ultra-performance liquid chromatograph from Waters, Milford, MA, USA. The UHPLC-MS procedure was performed following the methods followed by Idris and colleagues (Idris et al., 2024). Data processing and acquisition was performed under MS^E using MassLynx™ software version 4.1 (Waters, Milford, MA, USA) and the format was converted from project files (.PRO) to NetCDFfiles (.CDF) using Databridge in MassLynx and MZmine (Version 3). To specifically detect phytochemical compounds, ionization was in negative mode and the temperature of desolvation was set at 275 °C (650 L/h) and voltage at 15 V. The compounds were identified both in MS^E mode and in resolution mode (between the range of *m/z* 150–1500). In MS^E mode, data was captured at a low collision of 4 V and then at a higher collision energy range (40–100 V) to also obtain fragmentation data. Sodium formate was used to calibrate the instrument and Leucine enkephalin was a reference for mass determination accuracy. Waters T3 HHS, 2.1 × 150 mm, 1.7 μm column was used.

During separation, 0.1 % formic acid in water (solvent A) and 0.1 % formic acid in acetonitrile (solvent B) were used for mobile phase with 2 μL volume initially injected. The flow was linear, and the flow rate was set at 0.3 mL/min. The flow was maintained for 22 min with solvent A flowing for 1 min at 100 % gradient to 28 % for solvent B which was then raised to 40 % for 50 s. A wash step was then performed for 1.5 min at 100 % solvent B after-which the instrument was re-equilibrated for 4 min at 55 °C. At MS^E acquisition mode, retention time (RT) was set to start from 0.0 to 29.0 min and tolerance at ±0.2 min while *m/z* tolerance was set at 0.01 or 10ppm. Adducts in the negative ion ($[M-H]^-$, $[M-2H]^{2-}$, $[M-H-H_2O]^-$, $[M+Cl]^-$, $[M-H-CO_2]^-$, $[M+HCO_2]^-$, and [2M-H]) were considered. Mass range was 40–1200 Da and the mass accuracy tolerance was set at 5 ± 5 ppm. Detection of compounds was done according to UV, MS1, MS2 (*m/z*) and RT. Compounds were predicted according to the N-rule and the seven heuristic rules. The selection of the spectra was performed, and the retention times were aligned during the identification of metabolites. Unknown compounds were grouped, and their compositions were predicted. Compounds were named tentatively using 3 steps: 1) The masses of the compounds were matched and compared to existing data in Metlin (http://metlin.scripps.edu/index.

php (accessed on 15 October 2023), MassBank (http://www. MassBank.jp) (accessed on 15 October 2023), NIST (http://chemdata.nist.gov/ (accessed on 15 October 2023), and ReSpect (http://spectra.psc.riken.jp/(accessed on 15 October 2023). 2) Compounds were identified by comparing their mass fragmentation, retention time and ionization modes to existing phenolic compounds standards run at the same conditions. Due to the presence of many compounds identified in this present study, not all standards were used. For other compounds, theMS^1 and MS^2 fragment ions were obtained from previous literature and databases. 3) The calculation of carbons atoms at the peak of compounds with several isotopes was done to limit false identifications.

2.3.1. Specificity and sensitivity

Phenolic compounds such as epicatechin and catechin were run at the same conditions and used as standards for the detection of phenolic compounds in the plant extract. This study did not focus on specific phenolic compounds, leading to many compounds detected. Due to too many compounds detected, not all standards were used. However, the MS^1 and MS^2 fragment ions of previous similar compounds were found in databases and used to determine the detected compounds.

The sensitivity of the method used in this study was validated in a previously similar study (Idris et al., 2024). In brief, the limits of detection (LODs) and limits of quantification (LOQs) were used calculated and chemical markers were set. A UV and concentration standard curve for calibration was generated from epicatechin and catechin standards at 3.9; 7.8; 15.6; 62.5; 125.0 and 250,0 mg/L concentrations. The intra (0.14−3.14 %) and inter (1.01−2.90 %) repeatability of the RT of standards ranging from was considered. Phenolic acids were detected at 300, 309, and 322 nm and flavonols flavanols were detected at 254, 255, and 354, and 278 nm, respectively. The correlation coefficient of linear regression was maintained at $r > 0.99$.

2.4. Flavonol

Quercetin was used as a standard to determine the concentration of flavonols, and the quantity of flavonol was expressed as mg quercetin equivalent (QE) per gram of the extract (mg QE/g). The standard and samples were plated in a 96-well plate with 12.5 μL of 0.1 % HCl and 225 μl of 2 % HCl. The plate was incubated at room temperature for 30 min before reading at 360 nm in a Multiskan Spectrum plate reader (Thermo Fisher Scientific, Waltham, MA, USA) (Matsabisa et al., 2022).

2.5. Flavanol

Catechin (1 mM) was used as a standard to quantify the amount of flavanol in the extract. A volume of 25 μL of samples and the standard were plated into a 96-well plate after which 275 μl DMACA solution (DMACA in methanol-HCl to a concentration of 10 μg/mL) was added. The plate was kept at room temperature for 30 min before reading. Absorbance was read at 640 nm. Results were expressed as mg catechin equivalent (CE) per gram of the extract (mg CE/g) (Matsabisa et al., 2022).

2.6. Alkaloid

To detect the presence alkaloid, the sample (500 mL) was mixed with 2 M sodium phosphate buffer (pH 4.7), BCG solution (5 ml) and chloroform (12 mL). The presence of alkaloids was noticed by the presence of 2 layers (yellow and blue). If so, 0.1 mg/mL atropine (prepared in 2 M sodium phosphate buffer, pH 4.7) was used as a standard to calculate the concentration of alkaloid in the extract. The yellow layer in the extract sample/standard (300 μL) was plated into a 96-well plate and the plate was immediately read at 470 nm in a Multiskan Spectrum plate reader (Thermo Fisher Scientific, Waltham, MA, USA). Results were expressed as mg atropine equivalent (AE) per gram of the extract (mg AE/g) (Alabi et al., 2019).

2.7. Total polyphenols

Gallic acid was used as a standard in the quantification of total polyphenols. Both the standard and the extract sample (25 μL) were loaded in a 96-well plate. A concentration of 200 mM Folin-Ciocalteu reagent (125 μL) was then added in the wells containing the samples/standard after which sodium carbonate was added. After an incubation of 30 min at 37 °C, the plate was read at 765 nm in a Multiskan Spectrum plate reader (Thermo Fisher Scientific, Waltham, MA, USA). Results were expressed as mg gallic acid equivalent (GAE) per gram of the extract (mg GAE/g) (Mndi et al., 2023).

2.8. Trolox equivalent antioxidant capacity assay

Trolox equivalent antioxidant capacity (TEAC) of the plant extract was measured following the methods by Alabi and colleagues (Alabi et al., 2019). Briefly, Trolox (1000 mg/L) was used as a standard in the assay. Both the serial dilution concentrations prepared from Trolox, and the extract (25 μL) were added into wells of a 96-well plate in triplicates. Immediately after, 275 μL of 0.4 mg/mL 2,2-azino-bis-3-ethylbenzothiazolinee-6-sulphonic acid (ABTS) was added into the wells and the plate was kept at room temperature for 30 min before reading. The plate was read at 593 nm using a Multiskan Spectrum plate reader (Thermo Fisher Scientific, Waltham, MA, USA). Results were expressed as mg Trolox equivalent (TE) per gram of the extract (mg TE/g).

2.9. Ferric reducing antioxidant power assay

Ferric reducing antioxidant power (FRAP) assay of the plant extract was measured following the methods by Okaiyeto and colleagues (Okaiyeto et al., 2023). 1000 μM of vitamin C was diluted into a series of concentrations and used as a standard in the assay. A volume of 10 μL of the standard and extract were added into 96-well plate in triplicates. Immediately after, 300 μL of FRAP reagent solution (300 mM acetate buffer, pH 3.6, iron (III) chloride hexahydrate solution, and TPTZ solution in distilled water at 10:1:1:2 ratio) was added into each well and the plate was kept at room temperature for 30 min before reading. The plate was read using a Multiskan Spectrum plate reader purchased from Thermo Fisher Scientific, Waltham, MA, USA at 593 nm. Results were expressed as mg ascorbic acid equivalent (AAE) per gram of the extract (mg AAE/g).

2.10. 2,2-Diphenyl-1-picrylhydrazyl assay

The 2,2-diphenyl-1-picrylhydrazyl (DPPH) assay was performed following the methods by Okaiyeto and colleagues (Okaiyeto et al., 2023). Briefly, Trolox (1000 mg/L) was used as a standard in the assay to express the results as mg of Trolox per gram of the plant. Both the serial dilution concentrations prepared from Trolox, and the extract (25 μL) were added into 96-well plate in triplicates. Immediately after, 275 μL of 0.4 mg/mL DPPH was added into the wells and the plate was kept at room temperature for 30 min before reading. The plate was read at 593 nm using a Multiskan Spectrum plate reader (Thermo Fisher Scientific, Waltham, MA, USA). Results were expressed as mg Trolox equivalent (TE) per gram of the extract (mg TE/g).

2.11. Anti-inflammatory effect determination

Anti-inflammatory activity was determined by quantifying the amount of nitric oxide (NO) produced by RAW 264.7 cells treated

with the extract. A macrophage cell line (RAW 264.7 cells) from mice was used to determine anti-inflammatory activity. The cells were grown overnight in a 96-well plate (1×10^5 per well), in RPMI1640 culture medium supplemented with 10 % FBS. After the overnight incubation, the culture media was removed and cells were treated with different concentrations of the plant extract (50, 100 and 200 μg/mL) prepared in the culture media. The extract concentrations were chosen from a preliminary trial with consideration of the highest concentration that caused less toxicity. Positive control cells were treated with 100 μM aminoguanidine (AG). A volume of 50 μL of 1 μg/mL lipopolysaccharide (LPS) prepared in the media was then added to the cells and4 the plate was incubated for 24 h. NO production was determined by measuring the concentration of nitrite in the each well using the Griess reagent. A volume of 50 μL of the spent medium from the plate was added into the wells of a new plate after which 50 μL of sulphanilamide solution (1 % sulphanilamide in 5 % phosphoric acid) was added. After a 10 min incubation in the dark at room temperature, the plate was read at 540 nm in a spectrophotometer (BioTek® PowerWave XS from Winooski, VT, USA). Sodium nitrite was used as a standard and the concentration of nitrite was measured in μM. The MTT assay was also performed to determine the toxicity of the extract concentrations as a function of the NO production (van de Venter et al., 2008).

2.12. Glucose and lipid metabolism

2.12.1. Glucose utilisation

Glucose utilisation was measured on treated hepatocarcinoma cells (C3A). The cells were maintained in complete medium prepared by adding 10 % FBS, 1 % Pen-Strep to MEM with 1 % NEAA in a 10 cm culture dish. A volume of 100 μL of the C3A hepatocarcinoma cells were then seeded in 96-well plates at a density of 2×10^4 cells/well and left overnight to attach. The cells were then treated with the extract concentrations (15.625, 31.25, and 62.5 μg/mL) prepared in the complete medium for 24 h before the cells were transferred to a new 96-well plate and the medium was removed. The cells were washed with PBS (100 μL) and 25 μL of incubation buffer prepared by diluting RPMI-1640 with PBS in 0.1 % BSA to a final glucose concentration of 8 mM and incubated for 4 h. Glucose oxidase (200 μL) was added into the cells and the 96-well plate was incubated for 15 min at room temperature before reading at 510 nm using a BioTek® PowerWave XS spectrophotometer (Winooski, VT, USA) (van de Venter et al., 2008).

2.12.2. Glucose uptake

C3A hepatocarcinoma cells were maintained in complete medium prepared by adding 10 % FBS, 1 % Pen-Strep to MEM with 1 % NEAA in a 10 cm culture dish and then seeded in wells of a 96-well plate (100 μL of 2×10^4 cells/well) overnight. The cells were then treated with the extract concentrations ((15.625, 31.25, and 62.5 μg/mL) prepared in the complete medium for 24 h. The cells were then transferred to another 96-well plate where 200 μL of glucose oxidase prepared from 1 mU/mL *Aspergillus niger* glucose oxidase, 2.5 U/mL horseradish peroxidase, 0.25 mM EDTA, 3 mM phenol, 0.5 M PBS, pH 7.0, and 0.4 mM 4-aminoantipyrine, was added. The standard contained only glucose, medium and the buffer without cells. The plate was kept at room temperature for 15 min and then read in a BioTek® PowerWave XS spectrophotometer (Winooski, VT, USA) at 510 nm. Glucose intake (in mM) was measured by finding the difference between the glucose concentration in the standard and the glucose remaining in the samples after the reaction (van de Venter et al., 2008).

2.12.3. Cytotoxicity

The MTT assay was performed after the glucose uptake and utilisation assays. After both assays, the medium was removed, and the cells were treated with 100 μL of complete medium with 0.5 mg/mL MTT followed by a 1-hour incubation at 37 °C. The MTT solution was then aspirated, and DMSO (100 μL) was added to the wells containing the cells. The plate was read using a BioTek® PowerWave XS spectrophotometer (Winooski, VT, USA) at 540 nm (van de Venter et al., 2008).

2.12.4. Lipase inhibition

Lipase inhibition was determined following the methods by Pringle and colleagues (Pringle et al., 2021). Briefly, 10 μL of extract concentrations (31.25, 62.5, 125, 250, 500 μg/mL) prepared in 100 mM Tris−HCl, pH 8.0 were aliquoted into wells in quadruplicate of a 96-well plate. The concentrations were prepared from the highest soluble concentration to the lowest concentration that at least showed lipase inhibition activity. A volume of 40 μL Porcine lipase enzyme was then added into the wells containing the extract solutions. The plate was kept at 37 °C for15 min. A volume of 170 μL of the 1 mg/mL *p*-nitrophenyl palmitate (pNPP) substrate (diluted in isopropanol) was added and the plate was incubated again at 37 °C for 25 min. The plate was then read in a BioTek® PowerWave XS spectrophotometer (Winooski, VT, USA) at 405 nm.

2.12.5. α-glucosidase inhibition

Following the methods of Kwon and colleagues (Kwon et al., 2006), α-glucosidase inhibition of the plant extract was measured against acarbose, as a standard. Both the standard and concentrations (0.1, 0.2, 0.3, 0.4, 0.5 mg/mL) of the plant prepared in distilled water were plated into a 96-well plate in triplicates up to 50 μL. The extract concentrations were chosen following the dilution series of α-glucosidase concentrations used and reported from previous studies (Telagari and Hullatti, 2015). A volume of 100 μL of α-glucosidase was then added to each well. The plate was incubated for 10 min at room temperature. A volume of 50 μL of the substrate (5 mM of 4-nitrophenyl beta-d-glucoside (pNPG) in 20 mM phosphate buffer, pH 6.8) was the added to the wells and the reaction was allowed to occur for 30 min at 35.5 °C. The plate was read at 405 nm using a Multiskan Spectrum plate reader (Thermo Fisher Scientific, Waltham, MA, USA).

2.13. Statistical analysis

Data was analysed using Prism version 5 (GraphPad software). A non-parametric test was done using One-Way ANOVA and the Turkey post-test with the value of ($P < 0.05$) indicating significance. The significance in the data is indicated by letters of the alphabet, with different letters showing significance between groups and the same letters denoting no significance between groups.

3. Results

3.1. Cytotoxicity

The toxicity of the aqueous extract of *A. johnsonii* leaves was investigated against C3A hepatocarcinoma cells and the results are shown in Fig. 1. Melphalan was used as a positive control and successfully showed a significant ($P < 0.05$) decrease of 93.95 % in cell viability in the untreated C3A cells compared to the negative control cells (100 % cell viability). Cell viability in the cells treated with the extract was concentration dependent, with the lower concentrations (15.625, 31.25, 62.5, and 125 μg/mL) showing significantly ($P < 0.05$) higher cell viability compared to the negative control cells. The higher concentrations (200 and 250 μg/mL) reveal the possible cytotoxicity of the plant extract as shown by a significant ($P < 0.05$) decrease in cell viability with the highest concentration showing almost 50 % decrease in cell viability compared to control cells.

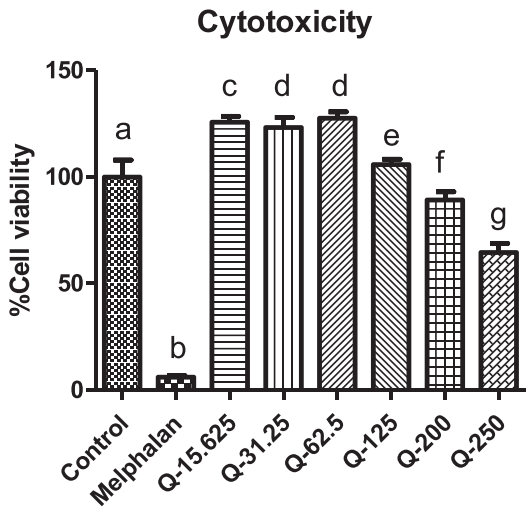

Fig. 1. Toxicity of different concentrations (15.625, 15.625, 31.25, 62.5, 125, 200, and 250 μg/mL) of the *A. johnsonii* aqueous leaf extract and Melphalan (10 μM) against C3A hepatocarcinoma cells after 48 h. The bar graph is a result of the mean of values in quadruplicate with error bars representing standard deviation. Data was analysed using One-way ANOVA and Tukey post-test. The letters on top of the bars indicate significance, and significant difference is shown by different letters ($P < 0.05$).

3.2. Ultra-high performance liquid chromatography mass spectrometry (UHPLC-MS) analysis

Phytochemical screening of the aqueous leaf extract of *A. johnsonii* identified a total of 34 phenolic compounds in the extract as depicted Table 1. The chromatograph obtained from the phytochemical screening is shown in Fig. 2. Flavonoids (flavonols, flavanols and flavones) were the most abundant phenolic compounds identified in the plant extract amongst other compounds such as hydroxybenzoic acids, gallotannins, quinic acid, citric acid and trihydroxy-octadecadienoic acid.

3.2.1. Identification of hydroxybenzoic acid and derivatives

In Fig. 2, peak 7 was identified as gallic acid whose *m/z* value is consistent with earlier studies owing to UV absorption of about 276 nm and *m/z* 125 [gallic acid $-H_2O-CO_2]^-$. Its derivatives were identified at peaks 6 and 7. Peak 6 was identified as 5-galloylquinic acid with *m/z* 343.0566 $[M-H]^-$, and MS^2 fragments *m/z* 191.0440 [M -H -galloyl]$^-$, *m/z* 169.0091 [M -H $-191]^-$ consistent with literature (Bresciani et al., 2017). Similarly peak 9 was identified as 3-galloylquinic acid. The order of elution and thus the loss of the galloyl group (G) is 5-G>3-G.

3.2.2. Identification of hydroxycinnamic acid

Ferulic acid $[M-H]^-$, could be detected with an adduct $[M-Na]^-$, *m/z* 215.0231 and it characteristic MS^2 fragment *m/z* 174.0336 $[M-H-H_2O]^-$, *m/z* 165.0247[feruloyl-CO]$^-$ and these results were tabulated in Table 1.

3.2.3. Identification of flavonols

Five flavonols could be detected and identified (peaks 27, 28, 29, 30 and 31 of Fig. 2). They were identified at characteristic uv maximum of 352 or 354 nm. Quercetin hexoside at peak 30 exhibited parent ion at *m/z* 463.0855 and MS^2 fragments *m/z* 300.9797 signifying loss of sugar moiety (−162). Additional acylation of quercetin hexoside with a galloyl group could result in quercetin-3-O-β-d-(6^{11}-galloyl) glucopyranoside and quercetin-3-O-β-d-(6^{11}- galloyl) galactopyranoside at peaks 27 and 28, respectively, identified using their order of retention on the column. Rutin was identified at peak 29 with parent ion 609.1478 $[M - H]^-$ and MS^2 fragment *m/z* 300.0137 [M -H-glc - rha - H]$^-$, i.e., consecutive loss of glucose (glc) (162 Da) and rhamnose (rha) (146 Da) sugars. The acetyl hexoside conjugate derivative of quercetin was identified at peak 31.

3.2.4. Identification of flavone

Two flavone peaks could be detected and identified (peaks 32 and 33 of Fig. 2). They could exhibit characteristic maximum wavelength of 341 nm. These included luteolin-7-galactoside with 447.0903 $[M-H]^-$ and its MS^2 fragments *m/z* 285.0282, [M- H -Glc]$^-$ *m/z* 171.0058 and nicotiflorin, *m/z* 593.1525 [M- H]-, its MS^2 fragments *m/z* 285.0388 [M- glc- rha- H]$^-$.

3.2.5. Identification of flavan-3-ols

Eleven flavan-3ols, including oligomeric flavan-3-ols were identified and depicted in Fig. 2 and Table 1. A few of them were in oligomeric/ polymerised forms (peaks 10, 11, 12, 15, 16, 17, 18, 19, 20, 24, 26) were identified from the stereoisomers; catechin and epicatechin and (Table 1). The monomers: catechin, epicatechin, gallocatechin and gallo(*epi*)catechin gave various lengths of polymers called proanthocyanidins (PAs). The two types of *B*-type PAs are linked by C4-C8 or C4−C6 interflavan linkages and *A*-type which have an additional C2−C5 or C2−C7 interflavan ether-linkages between the oligomers. The order of hydrophobicity for flavan-3ol monomers in the reversed-phase liquid chromatography ie (-/+)-epicatechin > (-/+)-catechin > (-/+)-epigallocatechin > (-/+)-gallocatechin also enabled identification of the monomers and the oligoners. The order of elution from the column is in the opposite direction. Thus (-/+)-gallocatechin elutes earlier and epicatechin comes out last. Therefore, (-/+)-gallocatechin (peak 11), and (-/+)-epicatechin (peak 17) could be identified. Catechin and epicatechin exhibit fragments *m/z* 151, 135 (due to retro Diels Alder (RDA) fragmentation) upon collision induced dissociation (CID) of their precursor ions $[M-H]^-$; *m/z* 289. In addition, fragment ions *m/z* 245 ([epicatechin -H-44]$^-$, loss of CO_2), *m/z* 205 ([epicatechin -H-84]$^-$, loss of flavonoid A ring) and *m/z* 179 ([M-H-110]$^-$, loss of flavonoid B ring) were consistent with that of literature (Escobar-Avello et al., 2019).

Some polymers of PAs such as B-type procyanidin trimer (*epi*)catechin-4,8′-(*epi*)catechin-4′,8″-(*epi*)catechin) (peak 10), (*epi*)catechin-(*epi*)gallocatechin (peak 12), procyanidin B1 dimer (also called B-type procyanidin dimer)- (Epi)catechin-4,8′- catechin (peak 15), procyanidin B11 dimer ((Epi)catechin-4,8′-(*epi*)catechin (peak 16) which is an isomer among others were formed from the interflavan linkages between different monomers. The main fragment ions of parent ions of procyanidin B1 dimer (B-type procyanidin dimer), i.e., (Epi)catechin-4,8′- catechin at *m/z* 577.1438 were *m/z* 425.0825 [M - H -152]$^-$from RDA of the heterocyclic rings, 407.0655 [M- H- 170]$^-$ from RDA of the heterocyclic rings and loss of water, *m/z* 289.0684 [M -H- 288]$^-$ from interflavanic bond cleavage, 451.1040 $[M + H - 126]^-$ from cleavages between C4−C5 and O−C2 of one of pyran rings.

Similarly, fragment ions of B-type procyanidin trimer with *m/z* 865.2118 and/ or 577.1343 included those at *m/z* 577.1438 [M - H −288]$^-$from interflavanic bond cleavage, *m/z* 695.1594 [M- H-170]$^-$ from RDA of the heterocyclic rings and loss of water, *m/z* 425.0729 [M- H- 288 - 152]$^-$ from interflavanic bond cleavage plus RDA of the heterocyclic rings, *m/z* 407.0655 [M- H- 288- 170]$^-$ from interflavanic bond cleavage and RDA of the heterocyclic rings and loss of water, etc. In addition, another main fragment ion *m/z* 577.1343 [M- H-290]$^-$might arise from interflavanic bond cleavage following the quinone-methide mechanism (Shui & Leong, 2004). Procyanidin B11 dimer may be characterised with *m/z* 575.0995.

3.2.6. Identification of gallotannins

Gallotannins constituted another significant group of phytochemicals to be identified. They were detected at peaks (13, 14, 21, 22, 23, and 25) in Fig. 2. The main HHDP galloyl glucose moiety could be detected at peak 21. They are ellagic acid derivatives in polyol form

Table 1
Compounds identified from the extract of *Androstachys johnsonii* Prain.

Peak No	RT, min	UV λ_{max} (nm)	*m/z* $[M-H]^-$	MS/MS	Tentative name
1	1.48		225.0510	179.0437, 131.0379	unidentified
2	1.62		215.0231$^{[m-Na]-}$	165.0247, 174.0336, 96.9604	Ferulic acid
3	1.72		191.0080	unfragmented	Quinic acid
4	1.80	225	191.0457	unfragmented	Citric acid
5	1.83	225	191.0459	85.0176	Isocitric acid
6	4.69	273	343.0566	191.0440, 169.0091	5-Galloylquinic acid
7	6.94	272	169.0052	125.0175	Gallic acid
8	11.93	273	647.2078	343.0649, 191.0471	Galloylquinic acid derivative
9	12.37	274	343.0596	169.0050, 175.9536	3-Galloylquinic acid
10	12.94	279	865.2118	323.1297, 695.1594	B-type procyanidin trimer ((Epi)catechin-4,8′-(*epi*)catechin-4′,8″-(*epi*) catechin)
11	13.23	273	305.0587	261.0300	(+)-Gallocatechin
12	13.96	277	593.1240	449.1241, 433.0793	(Epi)catechin-(*epi*)gallocatechin
13	14.17	274	495.0747	169.0009, 125.0170, 325.0498, 343.0668	Mucic acid lactone digallate
14	14.24	274	495.0744	345.0760, 203.0758	Mucic acid lactone digallate isomer
15	15.43	279	577.1438	289.0684, 125.0148, 425.0825, 407.0655, 451.1040	Procyanidin B1 dimer (B-type procyanidin dimer)-(Epi)catechin-4,8′- catechin
16	15.91	279	577.1367	289.0710, 425.0725, 125.0126, 407.0942	Procyanidin B11 dimer ((Epi)catechin-4,8′-(*epi*)catechin
17	16.25	279	289.0624	245.0777	(Epi)catechin
18	16.28	279	579.1522	289.0627	Procyanidin B4 (Catechin-4,8′-(*epi*) catechin)
19	16.48	279	865.2097	289.0622, 325.0828	Procyanidin trimer ((Epi)catechin-4,8′-(*epi*) catechin-4′,8″-(*epi*)catechin (isomer))
20	16.86	279	865.2111	291.0057, 575.0995	Procyanidin trimer (Epi)catechin-4,8′-(*epi*) catechin-4′,8″-(*epi*)catechin (isomer))
21	17.79	268	633.0814	463.0589, 300.9778	HHDP galloyl glucose isomer.
22	17.95		647.0881	305.0703, 485.0419, 633.0795	Methyl galloyl-HHDP-hexose
23	18.43	277	951.0864	300.9938, 475.0364, 169.0060, 125.0157	Trisgalloyl HHDP glucose isomer
24	19.49	279	577.1343	289.0629, 425.0729	Procyanidin B5 Catechin-4,8′-(*epi*)catechin (isomer)
25	20.38	276	953.1051	476.0410, 541.2192 300.9952, 169.0020, 463.0730	Galloyl chebuloyl -HHDP glucose
26	20.80	278	595.1254	541.2440, 481.1049, 385.1217	(Epi)gallocatechin-(*epi*)catechin
27	21.10	266, 353	615.1038	300.0220, 463.1964	Quercetin 3-O-β-d-(6^{11}-galloyl) glucopyranoside
28	21.36	264, 354	615.1016	537.2035, 463.0755	Quercetin 3-O-β-d-(6^{11}-galloyl) galactopyranoside
29	21.67	256, 354sh	609.1478	300.0137	Rutin (Quercetin 3-O-(6-O-rhamnosyl-glucoside))
30	22.19	254sh, 352	463.0855	300.9797	Quercetin hexoside
31	22.83	268sh, 352	761.1660	549.2669, 505.2141, 485.1760, 300.9898	Quercetin O-acetyl Hexoside derivative
32	23.20	266, 341	593.1525	300.9981, 285.0388	Nicotiflorin
33	23.75	266, 341	447.0903	285.0282, 171.0058	Luteolin 7- O -glucoside
34	24.60		327.2097	215.1185, 211.1227	Trihydroxy-octadecadienoic acid

HHDP = hexahydroxydiphenic acid, $^{[m-Na]-}$=$[M-Na]^-$, sh = shoulder.

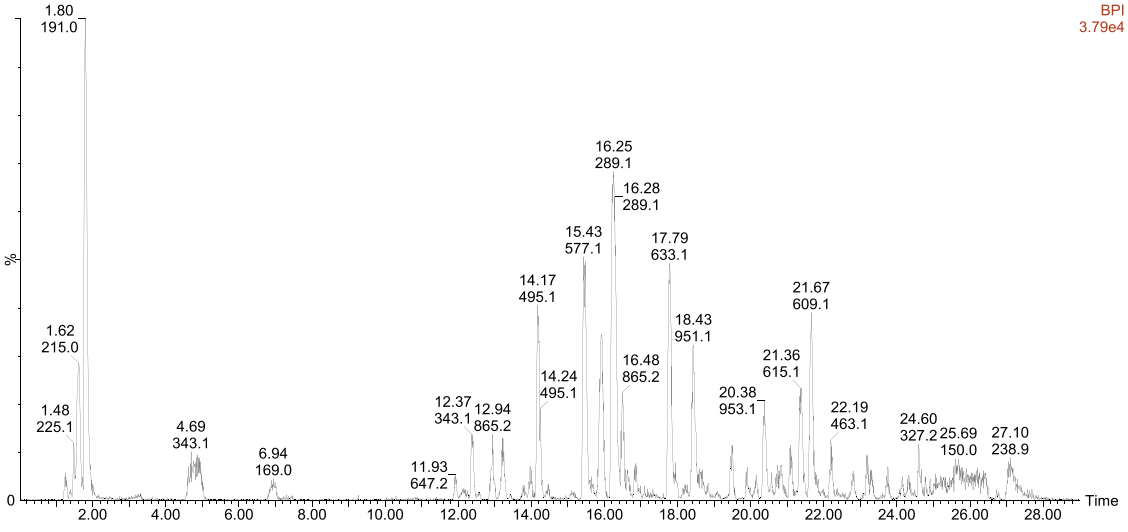

Fig. 2. *Androstachys johnsonii* Prain aqueous leaf extract UHPLC-ESI-MS base peak chromatogram obtained after analysis in the ESI negative mode.

distinguished by their characteristic fragment ion in their spectra leading to sequential losses of galloyl (−152 Da), gallate (170 Da), and HHDP residues (301 Da) (Singh et al., 2016). HHDP-galloylglucose has a precursor ion of *m/z* 633.0814 $[M- H]^-$ and its MS^2 fragments 463.0589 $[M- H- galloyl- H-H_2O]^-$, 300.9778 $[M- H- galloyl-H_2O- Hex]^-$. Trisgalloyl HHDP glucose could be detected at *m/z* 951.0864 $[M- H]^-$, and its MS^2 fragment 300.9938 $[M- H- galloyl-H_2O- HHDP]^-$, 475.0364, 169.0060 [M - H -galloyl −191]$^-$, 125.0157 [gallic acid $-H_2O-CO_2]^-$. Mucic acid lactone digallate at peaks 13 and 14 could also be identified with *m/z* 495.0747 ($[M -H]^-$), 343.0668 [M -H- galloyl]$^-$, 169.0009 [M - H -galloyl −191]$^-$, 169.0009 [gallic acid -H]$^-$ and *m/z* 125.0170 [gallic acid $-H_2O-CO_2]^-$, while *m/z* 325.0498 signifies possibility of lactonisation.

3.2.7. Identification of other compounds

Other compounds like quinic acid, citric acid and trihydroxy-octadecadienoic acid using accurate mass match.

3.3. Phenolic compounds quantification and antioxidant capacity

It was deduced from the phytochemical profiling (Table 1) that flavonoids are majorly present in the aqueous leaf extract of *A. johnsonii*. Flavonoids (flavanol and flavonol) and alkaloids were quantified, and the results are shown in Table 2. In the total polyphenol content (403.28 ± 12.75 mg GAE/g), 88.35 ± 2.16 mg CE/g is consisted of flavanols and 6.96 ± 3.10 mg QE/g flavonol. No alkaloids were identified in the extract. Antioxidant capacity was determined by measuring DPPH, FRAP, and TEAC values, and the results are depicted in Table 2. The plant extract showed an overall high antioxidant capacity. The extract showed a higher FRAP value (1342.68 ± 3.41 mg AAE/g) compared DPPH (571.57 ± 0.55 mg TE/g) and TEAC (478.88±0.09 mg TE/g).

3.4. Anti-inflammatory activity of A. johnsonii

Anti-inflammatory activity was of the aqueous extract of *A. johnsonii* leaves was investigated on RAW macrophage cells and depicted in Fig. 3. The relative excessive production of nitrite represented increased inflammation in the macrophage cells. The negative control cells with no induction of inflammation by LPS showed a low production of nitrite (approximately 10 μM). All cell groups with induced inflammation through the administration of LPS (both treated and untreated) showed a significant ($P < 0.05$) increase in the production of nitrite (Fig. 3A). The administration of LPS with no extract or drug treatment caused a significant ($P < 0.05$) increase in the nitrite concentration to 40 μM. The treatment of the inflammation-induced macrophage cells with AG (a control drug) showed a significant ($P < 0.05$) reduction of nitrite concentration compared to the untreated inflammation-induced cells (a difference of approximately 15 μM). The nitrite-reducing capacity of the extract was concentration-dependent, with the lower concentrations showing a non-significant ($P > 0.05$) difference amongst each other and a significant ($P < 0.05$) decrease in nitrite concentration (50 and 100 μg/mL) compared to the untreated induced cells. The highest concentration (200 μg/mL) of the extract investigated significantly ($P < 0.05$) reduced the nitrite concentration to a concentration comparable to the treated cells. As the production of nitrite is dependent on the cell viability, the MTT assay was conducted, and the results are represented in Fig. 3B Cells induced with LPS showed a significant ($P < 0.05$) decrease in cell viability. Although there was no significant difference in cell viability between cells treated with 100 μg/mL and those treated with 200 μg/mL, there was a significant decrease in nitrite production with 100 μg/mL extract treatment compared to 200 μg/mL extract treatment.

Table 2
Antioxidant capacity values and phenolic compound quantities in *A. johnsonii* aqueous leaf extract.

Phenolic compound/antioxidant capacity	Presence (+/-)	Quantity/value
Phenolic compounds		
Flavonols (mg QE/g)	+	6.96 ± 3.10
Flavanols (mg CE/g)	+	88.35 ± 2.16
Alkaloids (mg AE/g)	–	0
Total polyphenols (mg GAE/g)	+	403.28 ± 12.75
Antioxidant capacity		
DPPH (mg TE/g)	+	571.57 ± 0.55
FRAP (mg AAE/g)	+	1342.68 ± 3.41
TEAC (mg TE/g)	+	478.88±0.09

3.5. The hypoglycaemic effect of A. johnsonii

3.5.1. Glucose utilisation and intake

The effect of the *A. johnsonii* aqueous leaf extract on glucose and lipid metabolism was investigated through the determination of glucose uptake and utilisation, α-glucosidase inhibition, and lipase inhibition, respectively. The results are depicted in Fig. 4. Fig. 4A shows the results of glucose uptake amongst the groups. There was a significant ($P < 0.05$) increase in glucose uptake following insulin treatment, compared to the control cells. However, there was a significant ($P < 0.05$) increase in glucose uptake after treatment with the highest concentration (62.5 μg/mL) of the extract compared to the lower extract concentrations (15.625 and 31.25 μg/mL), and the normal untreated cells (Fig. 4A). Glucose uptake facilitated by the highest concentration of the leaf extract was comparable to insulin-induced glucose uptake. As depicted in Fig. 4B, there was no significant ($P > 0.05$) difference observed between the lowest concentrations (15.625 and 31.25 μg/mL) of the extract investigated. However, the highest concentration (62.5 μg/mL) of the extract caused a significant ($P < 0.05$) increase in glucose utilisation compared to the control (insulin) and the lower concentrations of the plant. Although the MTT assay (Fig. 4C) showed a slight significant ($P < 0.05$) decrease in cell viability in cells treated with 62.5 μg/mL concentration of the extract, both glucose intake and glucose utilisation results were not affected by cell viability.

3.5.2. Pancreatic lipase and α-glucosidase inhibition

Pancreatic lipase inhibition results are represented in Fig. 4D The inhibitory activity of the different concentrations (31.25, 62.5, 125, 250, 500 μg/mL) of the extract was compared to that of 100 μM of orlistat. The control drug (orlistat) showed approximately 65 % inhibition of pancreatic lipase activity. There was no significant ($P > 0.05$) difference in pancreatic lipase inhibition amongst the different concentrations of the extract. There was a significantly ($P < 0.05$) lower inhibitory activity against the pancreatic lipase with the extract treatment concentrations compared to the control. The inhibitory activity of the extract against α-glucosidase was compared to the standard drug, acarbose and the results are shown in Fig. 4E. There was a concentration-dependent increase in the inhibitory activity of both the extract and acarbose. However, the inhibitory activity of the extract against α-glucosidase increased to the highest inhibition of 97.54 %, while the inhibitory activity of acarbose only increased to 41.82 %.

4. Discussion

Medicinal plants exert their effects in the treatment of disease through the activity of the constituent bioactive compounds (Dar et al., 2023). The resulting pharmacological effect of medicinal plants is dependent on the type of phytochemical compounds in the plant (Süntar, 2020). This study revealed and focussed on the presence of phenolic compounds in the leaves of *A. johnsonii*, and their role in potentially reducing hyperglycaemic, oxidative stress, and inflammation. Oxidative stress plays a crucial role in the development of DM

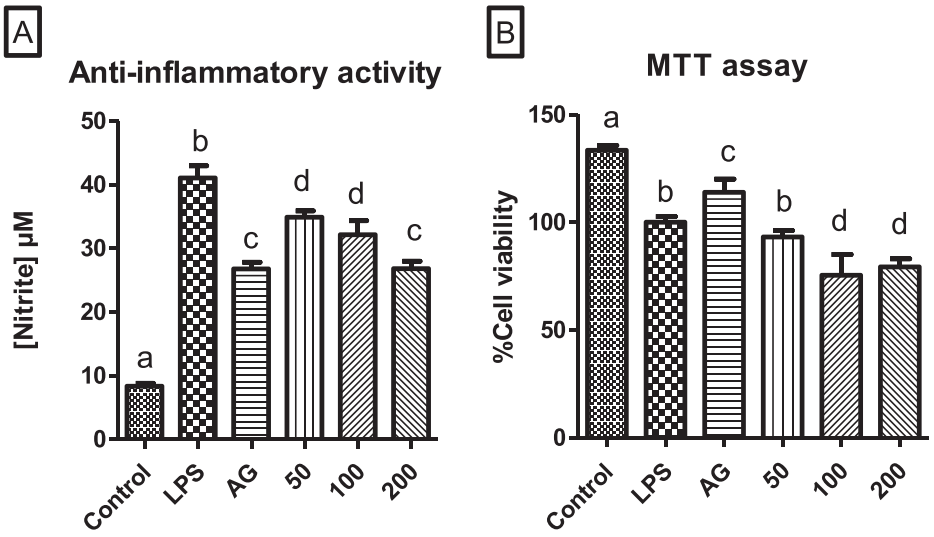

Fig. 3. A. The effect of *A. johnsonii* on the concentration of nitrite in LPS-activated macrophages after 24 h of exposure to treatments. Aminoguanidine (AG) was used as a control drug. B. Cell viability (%) of LPS activated macrophages after 24 h of exposure to treatments. The bar graph is a result of the mean of values in quadruplicate with error bars representing standard deviation. Data was analysed using One-way ANOVA and Tukey post-test. The letters on top of the bars indicate significance, and significant difference is shown by different letters ($P < 0.05$).

complications (Unuofin and Lebelo, 2020). In previous studies, diabetic models, characterised by hyperglycaemia showed excessive occurrence of reactive oxidative species and consequent organ damage (Abukhalil et al., 2021; Dong et al., 2022). Diabetic models have also shown the compromised antioxidant system caused by glucotoxicity (Rahmani et al., 2023). It is therefore a necessity to increase antioxidant capacity, in a hyperglycaemic state, to reduce oxidative stress. Phenolic compounds are bioactive compounds commonly known as free radical scavengers (Esmaeilzadeh Kenari and Razavi, 2022). The quantification of phenolic compounds in the leaves of *A. johnsonii* showed both the availability and abundance of polyphenols, specifically flavonoids.

Flavonoids are naturally occurring compounds found in fruits and vegetables and known for their beneficial effect in ameliorating oxidative stress (Shen et al., 2022). Quantified flavonols were further confirmed by the HPLC-MS detection of quercetin, a type of flavonol. Flavonols upregulate the antioxidant system by increasing the activation of antioxidant enzymes (catalase, superoxide dismutase, glutathione peroxidase, etc.) and upregulation of the expression of other non-enzymatic antioxidants (Shen et al., 2022).The present study has revealed the presence of phenolic acids (hydroxybenzoic and hydroxycinnamic acids) such as quinic acid, ferulic acid, gallic acid, and gallonylquinic acid. The detection of hydrocinnamic acid, ferulic acid, revealed the antioxidant capacity of *A. johnsonii* leaves. Ferulic acids are phenolic compounds with reported effect of reacting with DPPH and FRAP radicals, thereby reducing them (Yang et al., 2021a). The observed DPPH and FRAP scavenging capacityof the plant extract can therefore be linked to the presence of ferulic acid. Although ferulic acid is abundant in daily diet, its post-prandial bioavailability is insufficient (Mancuso et al., 2021). The aqueous leaf extract of *A. johnsonii* is therefore a necessary supplement in humans, especially in those with increased free radicals. The moiety and structure of gallic acid, with three phenolic hydroxyl groups contribute to its antioxidant effect (Yang et al., 2021a). Although a previous study has concluded that quinic acid lacks antioxidant capacity due to its stable cyclohexane structure and a missing aromatic ring, it has also revealed that quinic acid reduces lipid peroxidation in small amounts (Ercan and Doğru, 2022). The antioxidant capacity of the leaf extract of *A. johnsonii* can therefore be possibly alluded to a synergistic effect of the different phenolic acids present. The phenolic compound profiling of A. johnsonii in this study revealed the presence of new compounds such as mucic acid lactone digallate and luteolin 7-O-glucoside that have not been detected in previous profiling of the same plant, which could be beneficial in the amelioration of oxidative stress and inflammation.

Besides oxidative stress, diabetic complications are aggravated by the excessive accumulation of proinflammatory markers (Guo et al., 2022). For instance, complications such as nephrotic failure in diabetic patients can be detected through the increase in systemic immune-inflammation index (Guo et al., 2022). This finding suggests the occurrence and contribution of inflammation in the development of DM. Therefore, the reduction of proinflammatory cytokines plays a role in the management of diabetic complications (Guan et al., 2021). The process of inflammation is initiated by activation of IKb kinases as a response to an infection of tissue damage (Bai et al., 2021). The phosphorylation of the IKb kinases leads to the breakdown of NF-KB inhibitory proteins, allowing NF-KB to attach to the nucleus and initiate the expression of proinflammatory cytokines (Bai et al., 2021). Glucotoxicity caused by hyperglycaemia leads to the activation of the immune system through the increased transcription of the NF-KB gene and a downstream production and secretion of proinflammatory cytokines (Li et al., 2020). The excessive secretion of proinflammatory cytokines and inflammatory cell infiltration exacerbate insulin resistance in diabetic individuals, further increasing blood glucose levels (Zhao et al., 2024).

Besides other cytokines, the increase in the concentration of nitrite is an indicator of inflammation. In the present study, inflammation was induced by LPS, and observed by the increase in the level of nitrite as an indicator of nitric oxide production. It is evident that the induction of inflammation by LPS activation caused a significant ($P < 0.05$) decrease in cell viability. However, the type and concentration of treatment played a role in cell viability. Although inflammation is one of the factors that can lead to reduced cell viability, the reduction of nitrite after extract treatment was not necessarily caused by reduced cell viability. This is observed by the significant ($P < 0.05$) change in nitrite concentration between 100 μg/mL and 200 μg/mL concentrations of extract regardless of the non-significant ($P > 0.05$) difference in cell viability between the two concentrations. Treatment with the *A. johnsonii* aqueous leaf extract reduced the concentration of nitrite produced by the macrophage cells. Although the anti-inflammatory properties of *A. johnsonii* are not well-studied, individual phytochemical compounds detected in the leaf extract have been reported for their crucial role in amelioration of inflammation. Ferulic acid is associated with a significant reduction of pro-

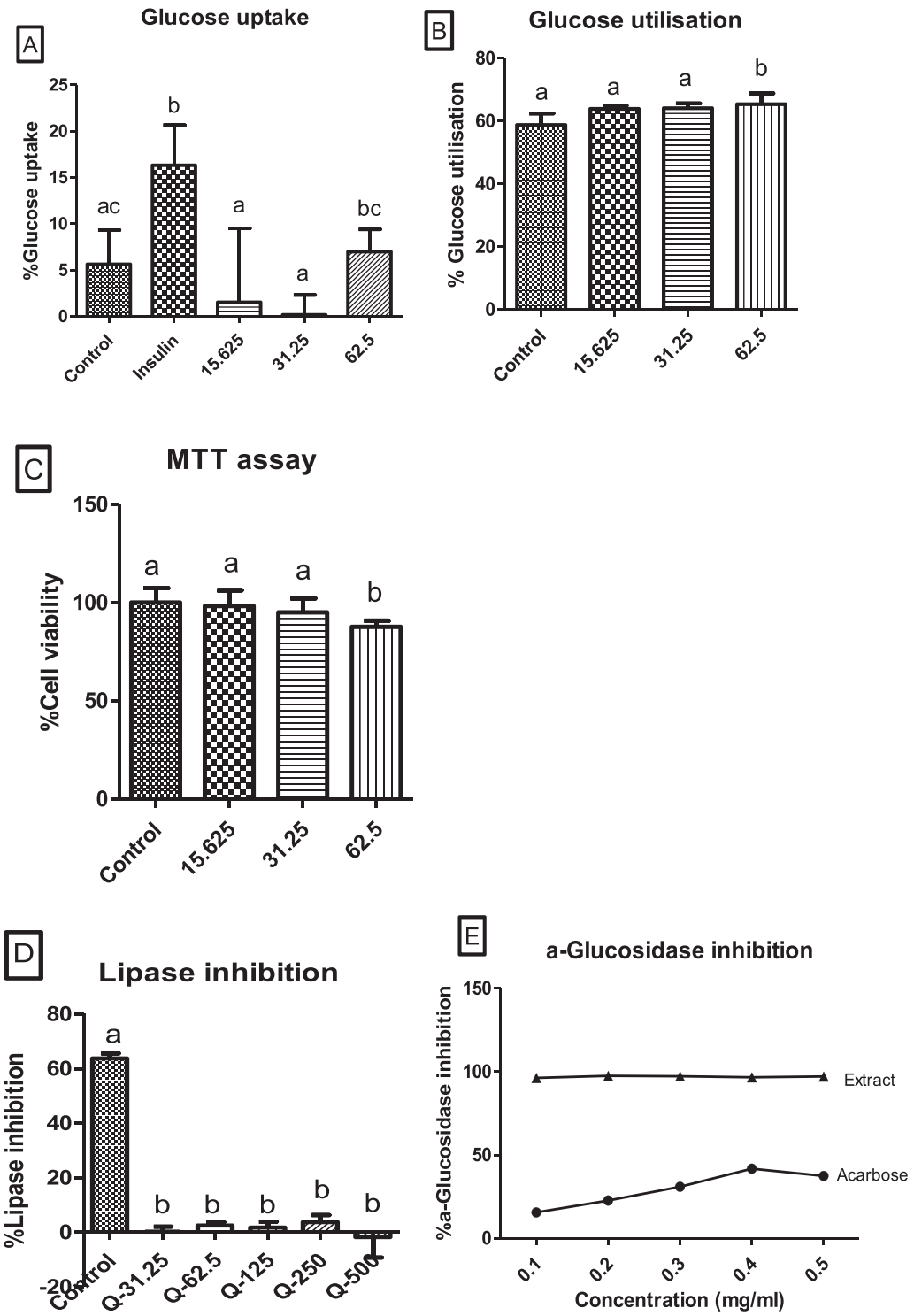

Fig. 4. The effect of different concentrations of *A. johnsonii* aqueous leaf extract on glucose and lipid metabolism. A. Glucose utilization (%) compared to insulin, in C3A cells after 24 h of treatment with different concentrations of the extract (in μg/mL unless stated otherwise). B. Glucose uptake (%) compared to insulin after 4 h of pre-treatment, in C3A cells. C. Glucose uptake and utilisation results were normalized to cell viability as determined using the MTT assay. D. Pancreatic lipase inhibition of the extract compared to orlistat (100 μM). E. The effect of the extract on α-glucosidase inhibition was compared to acarbose as a positive control. The bar graph is a result of the mean of values in quadruplicate with error bars representing standard deviation. Data was analysed using One-way ANOVA and Tukey post-test. The letters on top of the bars indicate significance, and significant difference is shown by different letters ($P < 0.05$).

inflammatory cytokines such as IL-6 and TNF-α (Liu et al., 2022a). This effect can be linked to the observed anti-inflammatory effect of the leaf extract of *A. johnsonii*. The anti-inflammatory effect of the extract can be linked to the presence of gallotannins, which were previously recorded for their anti-inflammatory activity through the upregulation of the AMPK pathway (Kim et al., 2022), and the downregulation of the NF-KB pathway (Chicas et al., 2020) which leads to the reduction of pro-inflammatory cytokines. The HPLC-MS profile detected the presence of gallic acid. Gallic acid exerts its anti-inflammatory properties by inhibiting the phosphorylation of IKb kinases, thereby blocking the expression of cytokines through down-regulation of NF-KB (Bai et al., 2021).

The role of obesity in the pathogenesis of DM is crucial. Lipid accumulation leads to insulin resistance and consequent hyperglycaemia. On the other hand, DM is a metabolic disease, and its pathogenesis involves impairment in lipid metabolism, which involves the excessive release of fatty acids. Previous studies have revealed the role of lipase inhibition in the management of both obesity and DM (Liu et al., 2020). In our present study, no lipase inhibitory activity was observed with the extract. However, some phytochemicals present in the leaf extract of *A. johnsonii* (flavonol, kaempferol, and quercetin) ameliorate dyslipidaemia (Jubaidi et al., 2021), by decreasing the level of triglycerides and low-density lipoprotein cholesterol and increasing high-density lipoprotein cholesterol (Abukhalil et al., 2021). It is therefore paramount to understand that although the extract shows no lipase inhibitory activity, its benefit in the reduction of hyperlipidaemia through possible alternative mechanisms cannot be ignored. The HPLC-MS profiling revealed the presence of anthocyanidins such as procyanidin B1 and B11. Besides their antioxidant properties, anthocyanins reduce the accumulation of lipids by decomposing cholesterol (Shen et al., 2022). This effect can reduce obesity and insulin resistance thereby alleviating hyperglycaemia.

The pathogenesis of DM arises from hyperglycaemia as a main characteristic (Galicia-Garcia et al., 2020). Both inflammation and oxidative stress are aggravated by glucotoxicity caused by the production of AGEs (Passarelli and Machado, 2021). The reduction of blood glucose is therefore a research interest in DM management. Blood glucose levels are controlled by the production and release of glucose into the blood, and glucose uptake by the cells (Norton et al., 2022). An increase in the activity of α-glucosidase ultimately leads to the rapid breakdown of carbohydrates and a release of excessive glucose molecules into the blood (Lawal et al., 2022). Similarly, the low uptake of glucose, mainly caused by insulin resistance leads to triglyceride breakdown and hyperglycaemia (Kalra et al., 2021). The hypoglycaemic effect of *A. johnsonii* was observed through the evident inhibition of α-glucosidase.

Flavonoids improve glucose transporter expression through the activation of the insulin pathway factors such as PI3K/Akt which leads to a reduction in blood glucose (Manavi et al., 2021). Although the glucose uptake effect of the extract is comparable to that of insulin, it is arguable that the synergistic effect of the extract with insulin in vivo could result in an increased glucose uptake. It has also been reported that procyanidins function similarly to insulin in the process of glucose intake (Manavi et al., 2021). The presence of different procyanidins in the extract could have possibly played a role in both glucose intake and utilisation, leading to a similar effect caused by insulin. Therefore, *A. johnsonii* extract is a possible alternative in the amelioration of insulin resistance.

5. Conclusion

Scientific focus on medicinal plant research aims to find more effective and affordable treatment for medical complications. In this current study, the aqueous leaf extract of *A. johnsonii* was found to cause a concentration-dependent reduction in inflammation and exhibit possible antioxidative effect as observed with antioxidant capacity values. The extract also showed a very high inhibitory activity against α-glucosidase compared to the standard drug (acarbose) The hypoglycaemic, anti-inflammatory and antioxidative effects observed in this study were linked to the phenolic compounds identified, with abundance of flavonoids. The observed effect of the plant extract is dependent on the concentration, with very high concentration showing cytotoxicity. It is therefore paramount to find the suitable concentration that is highly effective with lower cytotoxicity. These findings therefore serve as contribution towards further investigation of *A. johnsonii* as a possible pharmacotherapeutic medicinal plant in the treatment of DM.

6. Limitations and future perspectives

In this study, hepatocellular carcinoma cell lines were chosen due to their wide availability and high proliferation rates, which covers financial constraints. However, hepatocellular carcinoma cells display increased glycolysis and altered glucose utilisation which may have impacted the findings of this study. Future studies may consider the use of a different cell line to validate these results. In addition to this, the application of metabolomics in the cells could reveal more understanding on the glucose metabolism.

Funding

Funding for the research was obtained from Cape Peninsula University of Technology (grant number: CPUT RJ23).

Declaration of competing interest

The authors declare that they have no known competing financial interests or personal relationships that could have appeared to influence the work reported in this paper.

CRediT authorship contribution statement

Murendeni Nethengwe: Writing – original draft, Visualization, Software, Methodology, Investigation, Formal analysis, Data curation, Conceptualization. **Nasifu Kerebba:** Writing – review & editing, Data curation. **Kunle Okaiyeto:** Supervision, Conceptualization. **Chinyerum S. Opuwari:** Writing – review & editing, Supervision, Conceptualization. **Oluwafemi O. Oguntibeju:** Writing – review & editing, Visualization, Validation, Supervision, Resources, Project administration, Funding acquisition, Conceptualization.

Acknowledgement

The authors extend their acknowledgement to the Cape Peninsula University of Technology for financial support and research assistance.

References

Abukhalil, M.H., Althunibat, O.Y., Aladaileh, S.H., Al-Amarat, W., Obeidat, H.M., Al-khawalde, A.A.A., Hussein, O.E., Alfwuaires, M.A., Algefare, A.I., Alanazi, K.M., Al-Swailmi, F.K., Arab, H.H., Mahmoud, A.M., 2021. Galangin attenuates diabetic cardiomyopathy through modulating oxidative stress, inflammation and apoptosis in rats. Biomed. Pharmacother. 138, 111410. https://doi.org/10.1016/j.biopha.2021.111410.

Alabi, T.D., Brooks, N.L., Oguntibeju, O.O., 2019. Antioxidant capacity, phytochemical analysis and identification of active compounds in Anchomanes difformis. Nat. Prod. J. 10 (4), 446–458. https://doi.org/10.2174/2210315509666190422155347.

Amoo, S.O., Mudau, T.E., Olowoyo, J.O., 2022. In vitro α-glucosidase inhibitory activity of medicinal plants used traditionally for treating diabetes in Vhembe District, South Africa. J. Herbmed Pharmacol. 11 (4), 513–521. https://doi.org/10.34172/jhp.2022.59.

Andrade, C., Gomes, N.G.M., Duangsrisai, S., Andrade, P.B., Pereira, D.M., Valentão, P., 2020. Medicinal plants utilized in Thai Traditional Medicine for diabetes treatment: ethnobotanical surveys, scientific evidence and phytochemicals. J. Ethnopharmacol. 263, 113177. https://doi.org/10.1016/j.jep.2020.113177.

Bai, J., Zhang, Y., Tang, C., Hou, Y., Ai, X., Chen, X., Zhang, Y., Wang, X., Meng, X., 2021. Gallic acid: pharmacological activities and molecular mechanisms involved in inflammation-related diseases. Biomed. Pharmacother. 133, 110985. https://doi.org/10.1016/j.biopha.2020.110985.

Bhatti, J.S., Sehrawat, A., Mishra, J., Sidhu, I.S., Navik, U., Khullar, N., Kumar, S., Bhatti, G.K., Reddy, P.H., 2022. Oxidative stress in the pathophysiology of type 2 diabetes and related complications: current therapeutics strategies and future perspectives. Free Rad. Biol. Med. 184 (April), 114–134. https://doi.org/10.1016/j.freeradbiomed.2022.03.019.

Blahova, J., Martiniakova, M., Babikova, M., Kovacova, V., Mondockova, V., Omelka, R., 2021. Pharmaceutical drugs and natural therapeutic products for the treatment of type 2 diabetes mellitus. Pharmaceuticals 14 (8), 806. https://doi.org/10.3390/ph14080806.

Bodke, H., Wagh, V., Kakar, G., 2023. Diabetes mellitus and prevalence of other comorbid conditions: a systematic review. Cureus. https://doi.org/10.7759/cureus.49374.

Bouyahya, A., El Omari, N., Elmenyiy, N., Guaouguaou, F.-E., Balahbib, A., Belmehdi, O., Salhi, N., Imtara, H., Mrabti, H.N., El-Shazly, M., Bakri, Y., 2021. Moroccan antidiabetic medicinal plants: ethnobotanical studies, phytochemical bioactive compounds, preclinical investigations, toxicological validations and clinical evidences; challenges, guidance and perspectives for future management of diabetes worldwide. Trends. Food Sci. Technol. 115, 147–254. https://doi.org/10.1016/j.tifs.2021.03.032.

Bresciani, L., Martini, D., Mena, P., Tassotti, M., Calani, L., Brigati, G., Brighenti, F., Holasek, S., Malliga, D.-E., Lamprecht, M., Del Rio, D., 2017. Absorption Profile of (Poly)Phenolic Compounds after Consumption of Three Food Supplements Containing 36 Different Fruits, Vegetables, and Berries. Nutrients 9 (3), 194. https://doi.org/10.3390/nu9030194.

Cai, F., Chen, W., Zhao, R., Liu, Y., 2023. Mechanisms of Nrf2 and NF-κb pathways in diabetic wound and potential treatment strategies. Mol. Biol. Rep. 50 (6), 5355–5367. https://doi.org/10.1007/s11033-023-08392-7.

Chicas, M.C., Fang, C., Talcott, S., Talcott, S., 2020. Microbial metabolites of gallotannins suppress inflammation in RAW 264.7 macrophages through the modulation of the AMPK/NF-kb axis. Curr. Dev. Nutr. 4,. https://doi.org/10.1093/cdn/nzaa045_008 nzaa045_008.

Dar, R.A., Shahnawaz, M., Ahanger, M.A., Majid, I.U., 2023. Exploring the diverse bioactive compounds from medicinal plants: a review. J. Phytopharmacol. 12 (3), 189–195. https://doi.org/10.31254/phyto.2023.12307.

Dong, B., Shi, Z., Dong, Y., Chen, J., Wu, Z.-X., Wu, W., Chen, Z.-S., Han, C., 2022. Quercetin ameliorates oxidative stress-induced cell apoptosis of seminal vesicles via activating Nrf2 in type 1 diabetic rats. Biomed. Pharmacother. 151, 113108. https://doi.org/10.1016/j.biopha.2022.113108.

Ercan, L., Doğru, M., 2022. Antioxidant and antimicrobial capacity of quinic acid. Bitlis Eren Üniv. Bilimleri Dergisi 11 (4), 1018–1025. https://doi.org/10.17798/bitlisfen.1167047.

Escobar-Avello, D., Lozano-Castellón, J., Mardones, C., Pérez, A. J., Saéz, V., Riquelme, S., Von Baer, D., Vallverdú-Queralt, A., 2019. Phenolic Profile of Grape Canes: Novel Compounds Identified by LC-ESI-LTQ-Orbitrap-MS. Molecules 24 (20), 3763. https://doi.org/10.3390/molecules24203763.

Esmaeilzadeh Kenari, R., Razavi, R., 2022. Phenolic profile and antioxidant activity of free/bound phenolic compounds of sesame and properties of encapsulated nanoparticles in different wall materials. Food Sci. Nutr. 10 (2), 525–535. https://doi.org/10.1002/fsn3.2712.

Fenta, E.T., Eshetu, H.B., Kebede, N., Bogale, E.K., Zewdie, A., Kassie, T.D., Anagaw, T.F., Mazengia, E.M., Gelaw, S.S., 2023. Prevalence and predictors of chronic kidney disease among type 2 diabetic patients worldwide, systematic review and meta-analysis. Diabetol. Metab. Syndr. 15 (1), 245. https://doi.org/10.1186/s13098-023-01202-x.

Galicia-Garcia, U., Benito-Vicente, A., Jebari, S., Larrea-Sebal, A., Siddiqi, H., Uribe, K.B., Ostolaza, H., Martín, C., 2020. Pathophysiology of type 2 diabetes mellitus. Int. J. Mol. Sci. 21 (17), 6275. https://doi.org/10.3390/ijms21176275.

Guan, Y., Niu, H., Liu, Z., Dang, Y., Shen, J., Zayed, M., Ma, L., Guan, J., 2021. Sustained oxygenation accelerates diabetic wound healing by promoting epithelialization and angiogenesis and decreasing inflammation. Sci. Adv. 7 (35), eabj0153. https://doi.org/10.1126/sciadv.abj0153.

Guo, W., Song, Y., Sun, Y., Du, H., Cai, Y., You, Q., Fu, H., Shao, L., 2022. Systemic immune-inflammation index is associated with diabetic kidney disease in type 2 diabetes mellitus patients: evidence from NHANES 2011-2018. Front. Endocrinol. 13, 1071465. https://doi.org/10.3389/fendo.2022.1071465.

Haq, F.U., Siraj, A., Ameer, M.A., Hamid, T., Rahman, M., Khan, S., Khan, S., Masud, S., 2021. Comparative review of drugs used in diabetes mellitus—new and old. J. Diabetes. Mellitus. 11 (04), 115–131. https://doi.org/10.4236/jdm.2021.114009.

Idris, O.A., Kerebba, N., Horn, S., Maboeta, M.S., Pieters, R., 2024. Comparative phytochemistry using UPLC-ESI-QTOF-MS phenolic compounds profile of the water and aqueous ethanol extracts of Tagetes minuta and their cytotoxicity. South Afr. J. Bot. 164, 50–65. https://doi.org/10.1016/j.sajb.2023.11.035.

Jubaidi, F.F., Zainalabidin, S., Taib, I.S., Hamid, Z.A., Budin, S.B., 2021. The potential role of flavonoids in ameliorating diabetic cardiomyopathy via alleviation of cardiac oxidative stress, inflammation and apoptosis. Int. J. Mol. Sci. 22 (10). https://doi.org/10.3390/ijms22105094.

Kalra, S., Unnikrishnan, A.G., Baruah, M.P., Sahay, R., Bantwal, G., 2021. Metabolic and energy imbalance in dysglycemia-based chronic disease. Diab. Metab. Syndrome Obesity 14, 165–184. https://doi.org/10.2147/DMSO.S286888.

Khalid, M., Petroianu, G., Adem, A., 2022. Advanced glycation end products and diabetes Mellitus: mechanisms and perspectives. Biomolecules 12 (4), 542. https://doi.org/10.3390/biom12040542.

Khan, M.I., Bouyahya, A., Hachlafi, N.E.L., Menyiy, N.E., Akram, M., Sultana, S., Zengin, G., Ponomareva, L., Shariati, M.A., Ojo, O.A., Dall'Acqua, S., Elebiyo, T.C., 2022. Anticancer properties of medicinal plants and their bioactive compounds against breast cancer: a review on recent investigations. Environ. Sci. Poll. Res. 29 (17), 24411–24444. https://doi.org/10.1007/s11356-021-17795-7.

Kilicciogluı, I., Dulger, G., Senturk, F., Bozyel, M.E., Canli, K., Dulger, B., 2024. Chemical composition, antioxidant, antimicrobial and anticancer activities of endemic Cephalaria tuteliana. South Afr. J. Bot. 169, 231–241. https://doi.org/10.1016/j.sajb.2024.04.038.

Kim, H., Wang, Q., Im, Y., Yan, J., Kim, D., Kang, J.H., 2022. Anti-inflammatory effects of gallotannin in combination with Lactobacillus plantarum in a DSS-induced colitis mouse model. Curr. Dev. Nutr. 6, 298. https://doi.org/10.1093/cdn/nzac053.039.

Kwon, Y., Apostolidis, E., Shetty, K., 2006. A -amylase and a -glucosidase for management of. J. Food Biochem. 32 (2008), 15–31.

Lawal, T.A., Ononamadu, C.J., Okonkwo, E.K., Adedoyin, H.J., Shettima, M.L., Muhammad, I.U., Alhassan, A.J., 2022. In vitro and in vivo hypoglycaemic effect of Camellia Sinensis on alpha glucosidase activity and glycaemic index of white bread. Appl. Food Res. 2 (1), 100037. https://doi.org/10.1016/j.afres.2021.100037.

Li, C., Liu, X., Qiao, Y., Ning, L., Li, W., Sun, Y., Liu, D., Gao, W., Ma, C., 2020. Allicin alleviates inflammation of diabetic macroangiopathy via the Nrf2 and NF-kB pathway. Eur. J. Pharmacol. 876, 173052. https://doi.org/10.1016/j.ejphar.2020.173052.

Liu, T., Sun, L., Zhang, Y., Wang, Y., Zheng, J., 2022. Imbalanced GSH/ROS and sequential cell death. J. Biochem. Mol. Toxicol. 36 (1), e22942. https://doi.org/10.1002/jbt.22942.

Liu, T.-T., Liu, X.-T., Chen, Q.-X., Shi, Y., 2020. Lipase inhibitors for obesity: a review. Biomed. Pharmacother. 128, 110314. https://doi.org/10.1016/j.biopha.2020.110314.

Liu, Y., Shi, L., Qiu, W., Shi, Y., 2022b. Ferulic acid exhibits anti-inflammatory effects by inducing autophagy and blocking NLRP3 inflammasome activation. Mol. Cell Toxicol. 18 (4), 509–519. https://doi.org/10.1007/s13273-021-00219-5.

Magalhães, T.M., 2021. Effects of site and tree size on wood density and bark properties of Lebombo ironwood (Androstachys johnsonii Prain). N. Z. J. For. Sci. 51. https://doi.org/10.33494/nzjfs512021x32x.

Manavi, S.P., Amiri, T., Mozafaryan, M.J., 2021. Role of flavonoids in diabetes. J. Rev. Medic. Sci. 1 (3), 149–161. https://doi.org/10.22034/jrms.2021.366879.1016.

Mancuso, A., Cristiano, M.C., Pandolfo, R., Greco, M., Fresta, M., Paolino, D., 2021. Improvement of ferulic acid antioxidant activity by multiple emulsions: in vitro and In vivo evaluation. Nanomaterials 11 (2), 425. https://doi.org/10.3390/nano11020425.

Matsabisa, M.G., Bala, A., Tripathy, S., Digashu, M.M., Rautenbach, F., Dassarma, B., Erhabor, J.O., Braga, F.C., Mukherjee, P.K., Tang, M., Kang, Y., 2022. Study on South African indigenous teas—antioxidant potential, nutritional content, and hypoxia-induced cyclooxygenase inhibition on U87 MG cell line. Molecules 27 (11), 3505. https://doi.org/10.3390/molecules27113505.

Mfotie Njoya, E., Tabakam, G.T., Chukwuma, C.I., Mashele, S.S., Makhafola, T.J., 2024. Phytoconstituents of Androstachys johnsonii prain prevent reactive oxygen species production and regulate the expression of inflammatory mediators in LPS-stimulated RAW 264.7 macrophages. Antioxidants 13 (4), 401. https://doi.org/10.3390/antiox13040401.

Mndi, O., Sogoni, A., Jimoh, M.O., Wilmot, C.M., Rautenbach, F., Laubscher, C.P., 2023. Interactive effects of salinity stress and irrigation intervals on plant growth, nutritional value, and phytochemical content in mesembryanthemum crystallinum L. Agriculture 13 (5), 1026. https://doi.org/10.3390/agriculture13051026.

Molotja, G.M., Ligavha-Mbelengwa, M.H., Bhat, R.B., 2011. Antifungal activity of root, bark, leaf and soil extracts of Androstachys johnsonii Prain. Afr. J. Biotechnol. 10 (30), 5725–5727.

Nguyen, T.N., Yusuf, S., Chow, C.K., 2022. Availability and affordability of medicines for diabetes and cardiovascular disease across countries: information learned from the prospective urban rural epidemiological study. Diabetology 3 (1), 236–245. https://doi.org/10.3390/diabetology3010014.

Norton, L., Shannon, C., Gastaldelli, A., DeFronzo, R.A., 2022. Insulin: the master regulator of glucose metabolism. Metab. Clin. Exp. 129, 155142. https://doi.org/10.1016/j.metabol.2022.155142.

Okaiyeto, K., Kerebba, N., Rautenbach, F., Kumar Singh, S., Dua, K., Oguntibeju, O.O., 2023. UPLC-ESI-QTOF-MS phenolic compounds identification and quantification from ethanolic extract of Myrtus communis 'Variegatha': in vitro antioxidant and antidiabetic potentials. Arab. J. Chem. 16 (2), 104447. https://doi.org/10.1016/j.arabjc.2022.104447.

Passarelli, M., Machado, U.F., 2021. AGEs-induced and endoplasmic reticulum stress/inflammation-mediated regulation of GLUT4 expression and atherogenesis in diabetes mellitus. Cells 11 (1), 104. https://doi.org/10.3390/cells11010104.

Pieczykolan, A., Pietrzak, W., Gawlik-Dziki, U., Nowak, R., 2021. Antioxidant, anti-inflammatory, and anti-diabetic activity of phenolic acids fractions obtained from Aerva lanata (L.) Juss. Molecules 26 (12), 3486. https://doi.org/10.3390/molecules26123486.

Pringle, N.A., Van De Venter, M., Koekemoer, T.C., 2021. Comprehensive in vitro antidiabetic screening of *Aspalathus linearis* using a target-directed screening platform and cellomics. Food Funct. 12 (3), 1020–1038. https://doi.org/10.1039/D0FO02611E.

Rahman, Md.M., Dhar, P.S., Sumaia, Anika, F., Ahmed, L., Islam, Md.R., Sultana, N.A., Cavalu, S., Pop, O., Rauf, A., 2022. Exploring the plant-derived bioactive substances as antidiabetic agent: an extensive review. Biomed. Pharmacother. 152, 113217. https://doi.org/10.1016/j.biopha.2022.113217.

Rahmani, A.H., Alsahli, M.A., Khan, A.A., Almatroodi, S.A., 2023. Quercetin, a plant flavonol attenuates diabetic complications, renal tissue damage, renal oxidative stress and inflammation in streptozotocin-induced diabetic rats. Metabolites 13 (1), 130. https://doi.org/10.3390/metabo13010130.

Ramesh, P., Yeo, J.L., Brady, E.M., McCann, G.P., 2022. Role of inflammation in diabetic cardiomyopathy. Ther. Adv. Endocrinol. Metab. 13, 204201882210835. https://doi.org/10.1177/20420188221083530.

Rohm, T.V., Meier, D.T., Olefsky, J.M., Donath, M.Y., 2022. Inflammation in obesity, diabetes, and related disorders. Immunity 55 (1), 31–55. https://doi.org/10.1016/j.immuni.2021.12.013.

Saddique, F.A., Ahmad, M., Ashfaq, U.A., Muddassar, M., Sultan, S., Zaki, M.E.A., 2022. Identification of cyclic sulfonamides with an N-arylacetamide group as α-glucosidase and α-amylase inhibitors: biological evaluation and molecular modeling. Pharmaceuticals 15 (1), 106. https://doi.org/10.3390/ph15010106.

Sahakyan, G., Vejux, A., Sahakyan, N., 2022. The role of oxidative stress-mediated inflammation in the development of T2DM-induced diabetic nephropathy: possible preventive action of tannins and other oligomeric polyphenols. Molecules 27 (24), 9035. https://doi.org/10.3390/molecules27249035.

Shen, N., Wang, T., Gan, Q., Liu, S., Wang, L., Jin, B., 2022. Plant flavonoids: classification, distribution, biosynthesis, and antioxidant activity. Food Chem. 383, 132531. https://doi.org/10.1016/j.foodchem.2022.132531.

Shoukat, A., Imran, M., Khan, M.K., Ahmad, M.H., Ahmad, R.S., Ramadan, M.F., Nadeem, M., Yasmin, A., Rahim, M.A., Khan, M.I., 2024. Impact of spray drying operating conditions on yield, secondary metabolites, antioxidant potential and storage quality of grape (Vitis vinifera L.) pomace powder. South Afr. J. Bot. 169, 383–395. https://doi.org/10.1016/j.sajb.2024.04.035.

Shui, G., Leong, L. P., 2004. Analysis of polyphenolic antioxidants in star fruit using liquid chromatography and mass spectrometry. J. Chromatogr. A 1022 (1–2), 67–75. https://doi.org/10.1016/j.chroma.2003.09.055.

Singh, A., Bajpai, V., Kumar, S., Sharma, K. R., Kumara, B., 2016. Profiling of Gallic and Ellagic Acid Derivatives in Different Plant Parts of Terminalia arjuna by HPLC-ESI-QTOF-MS/MS. Natural Prod. Commun. 11 (2), 239–244.

Süntar, I., 2020. Importance of ethnopharmacological studies in drug discovery: role of medicinal plants. Phytochem. Rev. 19 (5), 1199–1209. https://doi.org/10.1007/s11101-019-09629-9.

Telagari, M., Hullatti, K., 2015. In-vitro α-amylase and α-glucosidase inhibitory activity of Adiantum caudatum Linn. And Celosia argentea Linn. extracts and fractions. Indian J. Pharmacol. 47 (4), 425. https://doi.org/10.4103/0253-7613.161270.

Unuofin, J.O., Lebelo, S.L., 2020. Antioxidant effects and mechanisms of medicinal plants and their bioactive compounds for the prevention and treatment of type 2 diabetes: an updated review. Oxid. Med. Cell Longev. 2020, 1–36. https://doi.org/10.1155/2020/1356893.

van de Venter, M., Roux, S., Bungu, L.C., Louw, J., Crouch, N.R., Grace, O.M., Maharaj, V., Pillay, P., Sewnarian, P., Bhagwandin, N., Folb, P., 2008. Antidiabetic screening and scoring of 11 plants traditionally used in South Africa. J. Ethnopharmacol. 119 (1), 81–86. https://doi.org/10.1016/J.JEP.2008.05.031.

Yang, J., Chen, J., Hao, Y., Liu, Y., 2021. Identification of the DPPH radical scavenging reaction adducts of ferulic acid and sinapic acid and their structure-antioxidant activity relationship. LWT 146, 111411. https://doi.org/10.1016/j.lwt.2021.111411.

Yang, Y., Vong, C.T., Zeng, S., Gao, C., Chen, Z., Fu, C., Wang, S., Zou, L., Wang, A., Wang, Y., 2021b. Tracking evidences of Coptis chinensis for the treatment of inflammatory bowel disease from pharmacological, pharmacokinetic to clinical studies. J. Ethnopharmacol. 268, 113573. https://doi.org/10.1016/j.jep.2020.113573.

Yao, X., Zhang, J., Zhang, X., Jiang, T., Zhang, Y., Dai, F., Hu, H., Zhang, Q., 2023. Age at diagnosis, diabetes duration and the risk of cardiovascular disease in patients with diabetes mellitus: a cross-sectional study. Front. Endocrinol. 14, 1131395. https://doi.org/10.3389/fendo.2023.1131395.

Ye, J., Wu, Y., Yang, S., Zhu, D., Chen, F., Chen, J., Ji, X., Hou, K., 2023. The global, regional and national burden of type 2 diabetes mellitus in the past, present and future: a systematic analysis of the Global Burden of Disease Study 2019. Front. Endocrinol. 14, 1192629. https://doi.org/10.3389/fendo.2023.1192629.

Zhao, L., Hu, H., Zhang, L., Liu, Z., Huang, Y., Liu, Q., Jin, L., Zhu, M., Zhang, L., 2024. Inflammation in diabetes complications: molecular mechanisms and therapeutic interventions. MedComm 5 (4), e516. https://doi.org/10.1002/mco2.516.